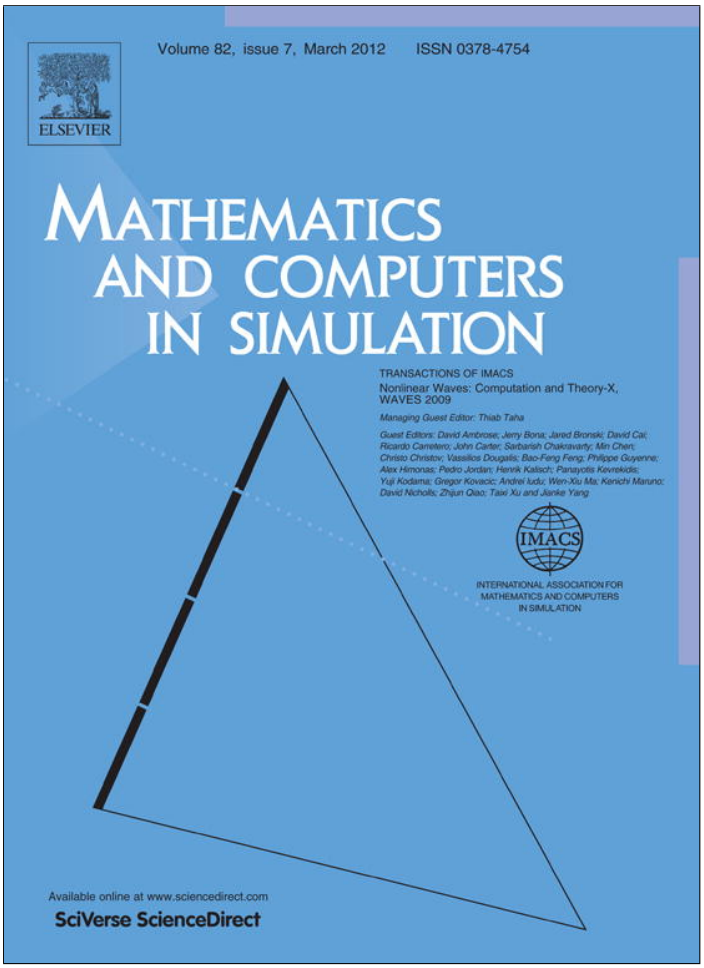

Available online at www.sciencedirect.com
ScienceDirect
Mathematics and Computers in Simulation 82 (2012) 1228–1238
MATHEMATICS AND COMPUTERS IN SIMULATION
www.elsevier.com/locate/matcom

Original Articles

Influence of the condensate and inverse cascade on the direct cascade in wave turbulence

A.O. Korotkevich [a,b,*]

[a] *Department of Mathematics and Statistics, MSC03 2150, 1 University of New Mexico, Albuquerque, NM 87131-0001, USA*
[b] *L.D. Landau Institute for Theoretical Physics RAS, 2 Kosygin Str., Moscow 119334, Russian Federation*

Received 7 November 2009; received in revised form 29 May 2010; accepted 7 July 2010
Available online 17 July 2010

Abstract

During direct numerical simulation of the isotropic turbulence of surface gravity waves in the framework of Hamiltonian equations formation of the long wave background or condensate was observed. Exponents of the direct cascade spectra at the different levels of an artificial condensate suppression show a tendency to become closer to the prediction of the wave turbulence theory at lower levels of condensate. A simple qualitative explanation of the mechanism of this phenomenon is proposed.

PACS: 47.27.ek; 47.35.−i; 47.35.Jk

Keywords: Wave turbulence; Condensate; Direct cascade

1. Introduction

Description of the water waves appeals scientists attention during several centuries. At the same time, first attempts to explain observed spatial and temporal spectra are relatively recent. One of the first and at the same time most famous works is the paper by Phillips [26] which was, probably, the first attempt to give an explanation for power-like spectra of surface gravity waves observed in numerous experiments. In just one decade statistical theory of water waves, based on the the kinetic equation for waves derived by Hasselmann [15] and solutions of this equation obtained from Zakharov's theory of wave (or weak) turbulence [33,41]. These solutions [37,41] are stationary Kolmogorov solutions of the kinetic equation corresponding to flux of energy from large to small scales (direct cascade) and flux of wave action (waves "number") from small to large scales (inverse cascade). Now the kinetic equation is a base tool for wave forecasting.

The Hasselmann kinetic equation for waves was derived under some assumptions, which include Gaussian statistics for the wave field and prevalence of resonant interactions [41]. These assumptions are subject to confirmation. Modern numerical methods allow us to perform wave field modeling in the framework of kinetic equations faster than the real processes in nature. At the same time, it is still not possible to create a wave forecasting model based on direct numerical simulation of the primordial dynamic equations. Fortunately, in practical applications we do not need to

* Correspondence address: Department of Mathematics and Statistics, MSC03 2150, 1 University of New Mexico, Albuquerque, NM 87131-0001, USA. Tel.: +1 505 277 2304; fax: +1 505 277 5505.
E-mail address: alexkor@math.unm.edu.

0378-4754/$36.00 © 2010 IMACS. Published by Elsevier B.V. All rights reserved.
doi:10.1016/j.matcom.2010.07.009

know velocity and elevation at every point of the surface. Statistics, especially mean wave height and speed, are what really matters for estimation of operational conditions of oil platforms and cargo ships. Such statistics are exactly the subject of the theory of weak turbulence. As a consequence, the problem of confirmation and correction of the theory of wave turbulence is of great practical importance.

Open sea observations confirm temporal and space spectra predicted by the theory of wave turbulence [8,16,30]. A comprehensive review of experiments and comparison with the theory of the weak turbulence can be found in [2,3,36]. At the same time even the most recent, state of the art wave tanks experiments give strange results [6,13], demonstrating dependence of the spectrum slope on the average steepness or forcing level.

One of the ways from this dead end is direct numerical simulation in the framework of dynamical equations. Such numerical experiments can be separated in two major groups. In swell simulation experiments initial condition is some spectral distribution, there is no pumping. Temporal evolution of such initial condition is simulated and than can be compared with corresponding simulation in the framework of kinetic equation [21,25,29,31,39,40]. More interesting and more complex is the simulation of the wave turbulence with pumping. Classical sandbox for such simulations is an isotropic turbulence, which allows us to demonstrate of the features of the wave turbulence and, at the same time, simplifies situation due to additional smoothing of the spectra after angle averaging. Although this situation looks pretty artificial, the isotropic turbulence can be observed in the sea with large amount of broken ice, for example, where waves create isotropic wave field after multiple reflections. But in such a case floating ice have to be taken into account, which makes situation more complex. Simulation of isotropic wave turbulence already confirmed some prediction of the theory of weak turbulence. Direct cascade spectra were obtained in [11,12,22]. Inverse cascade spectra, although in simplified equations, were obtained in [1]. For the first time simultaneous simulation of direct and inverse cascades for gravity waves in the framework of primordial dynamical equations was performed in [20]. Formation of the long wave background (condensate) due to inverse cascade flux was observed. The condensate development was influenced by the discreteness of the wavenumbers grid at the origin of the $\vec{k}$-space. Such discreteness is unavoidable in finite basin experiments with realistic size of experimental site corresponding to controllable weather conditions and reasonable wavemaker equipment.

Current paper is a continuation of the work [20], which was a brief declaration of the results of two initial numerical experiments (with fully developed and partially suppressed condensate). Although simulations explained some results of other authors [13,6], there was significant amount of questions which needed to be answered and for which only hints for solutions were proposed. The present article will concentrate on the condensate generation and its influence on the direct cascade spectra of wave turbulence of surface gravity waves. A more detailed and deep insight in the mechanism of the condensate influence is presented. Starting from the results of isotropic turbulence simulation author will explore in details how presence of the condensate changes the slope of direct cascade spectrum. It will be demonstrated that the presence of the inverse cascade is also important. At the same time, in the close to pure situation with suppressed both condensate and inverse cascade, observation shows spectrum slope close to previous numerous results of simulations [11,12,22]. A simple qualitative explanation of the mechanism of spectrum distortion is provided. Direct analysis of the simulation results supports the theory.

2. Theoretical background

Author follows previous works in theoretical description of the system under consideration [11,12,21,20].

2.1. Dynamical equations

We study the potential flow of an ideal inviscid incompressible fluid with the velocity potential $\phi = \phi(x,y,z;t)$:

$$\Delta\phi = 0,$$

in the infinitely deep domain occupied by the fluid. Equations for the boundary conditions at the surface are the following:

$$\left(\dot{\eta} + \phi'_x\eta'_x + \phi'_y\eta'_y\right)\Big|_{z=\eta} = \phi'_z\big|_{z=\eta}, \qquad \left(\dot{\phi} + \frac{1}{2}|\nabla\phi|^2\right)\Big|_{z=\eta} + g\eta = 0. \tag{1}$$

Here $\eta(x,y;t)$ is the surface elevation with respect to still water, g is the gravity acceleration. Eq. (1) are Hamiltonian [34] with the canonical variables $\eta(x,y;t)$ and $\Psi(x,y;t)=\phi(x,y,\eta(x,y;t);t)$:

$$\frac{\partial\eta}{\partial t}=\frac{\delta H}{\delta\psi},\qquad \frac{\partial\psi}{\partial t}=-\frac{\delta H}{\delta\eta}, \tag{2}$$

where H is the Hamiltonian of the system:

$$H=\frac{1}{2}\int_{-\infty}^{+\infty}dx\,dy\left(g\eta^2+\int_{-\infty}^{\eta}|\nabla\phi|^2\,dz\right),$$

Unfortunately H cannot be written in the close form as a functional of η and ψ. However, one can limit Hamiltonian by first three terms of expansion in powers of η and ψ:

$$\begin{aligned}
H&=H_0+H_1+H_2+\ldots,\\
H_0&=\frac{1}{2}\int\left(g\eta^2+\psi\hat{k}\psi\right)\,dx\,dy,\\
H_1&=\frac{1}{2}\int\eta\left[|\nabla\psi|^2-(\hat{k}\psi)^2\right]\,dx\,dy,\\
H_2&=\frac{1}{2}\int\eta(\hat{k}\psi)\left[\hat{k}(\eta(\hat{k}\psi))+\eta\,\Delta\psi\right]\,dx\,dy.
\end{aligned} \tag{3}$$

Here $\Delta=\partial^2/\partial x^2+\partial^2/\partial y^2$ is the Laplace operator, $\hat{k}$ is a linear integral operator ($\hat{k}=\sqrt{-\Delta}$), such that in k-space it corresponds to multiplication of Fourier harmonics:

$$\psi_{\vec{k}}=\frac{1}{2\pi}\int\psi_{\vec{r}}e^{i\vec{k}\vec{r}}\,d^2r,\qquad \eta_{\vec{k}}=\frac{1}{2\pi}\int\eta_{\vec{r}}e^{i\vec{k}\vec{r}}\,d^2r. \tag{4}$$

by $k=\sqrt{k_x^2+k_y^2}$. For gravity waves this reduced Hamiltonian describes four-wave interaction.

Then dynamical equations (2) acquire the form:

$$\begin{aligned}
\dot{\eta}&=\hat{k}\psi-(\nabla(\eta\nabla\psi))-\hat{k}[\eta\hat{k}\psi]+\hat{k}(\eta\hat{k}[\eta\hat{k}\psi])+\frac{1}{2}\Delta[\eta^2\hat{k}\psi]+\frac{1}{2}\hat{k}[\eta^2\Delta\psi]-\hat{F}^{-1}[\gamma_k\eta_k],\\
\dot{\psi}&=-g\eta-\frac{1}{2}\left[(\nabla\psi)^2-(\hat{k}\psi)^2\right]-[\hat{k}\psi]\hat{k}[\eta\hat{k}\psi]-[\eta\hat{k}\psi]\Delta\psi-\hat{F}^{-1}[\gamma_k\psi_k]+\hat{F}^{-1}[P_{\vec{k}}].
\end{aligned} \tag{5}$$

Here dot means time-derivative, $\hat{F}^{-1}$ is an inverse Fourier transform, γ_k is a dissipation rate (according to recent work [7] it has to be included in both equations), which corresponds to viscosity on small scales and, if needed, "artificial" damping on large scales. $P_{\vec{k}}$ is the driving term which simulates pumping on large scales (for example, due to wind). In the k-space supports of γ_k and $P_{\vec{k}}$ are separated by the inertial interval, where the Kolmogorov-type solution can be recognized. These equations were derived as a result of Hamiltonian expansion in terms of $\hat{k}\eta$. From the physical point of view the $\hat{k}$-operator is close to the derivative operator, so we expand in powers of the slope of the surface. In most of the experimental observations average slope of the open sea surface μ is of the order of 0.1, so such expansion is very reasonable.

These are dynamical equations which will be subject for modeling in a significant part of this article. In order to understand the motivation of the paper we need to introduce statistical description of the wave field.

2.2. Kinetic equation

For the analysis of the wave field it is natural to use the Fourier representation (4). Wave field functions $\psi(\vec{r},t)$ and $\eta(\vec{r},t)$ are real valued functions, so their Fourier transforms have Hermitian symmetry:

$$\psi_{\vec{k}}=\psi^*_{-\vec{k}},\qquad \eta_{\vec{k}}=\eta^*_{-\vec{k}}.$$

As a result we have two complex functions and each of them use effectively only half of the wavenumbers plane. For further derivation is is convenient to introduce so called normal variables:

$$a_{\vec{k}} = \sqrt{\frac{\omega_k}{2k}}\eta_{\vec{k}} + i\sqrt{\frac{k}{2\omega_k}}\psi_{\vec{k}}. \tag{6}$$

In this variables for a wave field of one plain wave with wavevector $\vec{k}_0$ only harmonics $a_{\vec{k}_0}$ will be nonzero. We can state that we introduced elementary excitations of the system. Hamiltonian equations in this variables has canonical form:

$$\dot{a}_{\vec{k}} = -i\frac{\delta H}{\delta a^*_{\vec{k}}}. \tag{7}$$

Hamiltonian in this terms allows us to separate different wave interaction processes:

$$\begin{aligned}
H_0 &= \int \omega_k |a_{\vec{k}}|^2 \, d\vec{k},\\
H_1 &= \frac{1}{6}\frac{1}{2\pi}\int E^{\vec{k}_0}_{\vec{k}_1\vec{k}_2}(a_{\vec{k}_1}a_{\vec{k}_2}a_{\vec{k}_0} + a^*_{\vec{k}_1}a^*_{\vec{k}_2}a^*_{\vec{k}_0})\delta(\vec{k}_1+\vec{k}_2+\vec{k}_0)\, d\vec{k}_1\, d\vec{k}_2\, d\vec{k}_0\\
&\quad + \frac{1}{2}\frac{1}{2\pi}\int C^{\vec{k}_0}_{\vec{k}_1\vec{k}_2}(a_{\vec{k}_1}a_{\vec{k}_2}a^*_{\vec{k}_0} + a^*_{\vec{k}_1}a^*_{\vec{k}_2}a_{\vec{k}_0})\delta(\vec{k}_1+\vec{k}_2-\vec{k}_0)\, d\vec{k}_1\, d\vec{k}_2\, d\vec{k}_0,\\
H_2 &= \frac{1}{4}\frac{1}{(2\pi)^2}\int W_{\vec{k}_1\vec{k}_2\vec{k}_3\vec{k}_4}(a_{\vec{k}_1}a_{\vec{k}_2}a_{\vec{k}_3}a_{\vec{k}_4} + a^*_{\vec{k}_1}a^*_{\vec{k}_2}a^*_{\vec{k}_3}a^*_{\vec{k}_4}) \times \delta(\vec{k}_1+\vec{k}_2+\vec{k}_3+\vec{k}_4)\, d\vec{k}_1\, d\vec{k}_2\, d\vec{k}_3\, d\vec{k}_4\\
&\quad + \frac{1}{4}\frac{1}{(2\pi)^2}\int F_{\vec{k}_1\vec{k}_2\vec{k}_3\vec{k}_4}(a^*_{\vec{k}_1}a_{\vec{k}_2}a_{\vec{k}_3}a_{\vec{k}_4} + a_{\vec{k}_1}a^*_{\vec{k}_2}a^*_{\vec{k}_3}a^*_{\vec{k}_4}) \times \delta(\vec{k}_1-\vec{k}_2-\vec{k}_3-\vec{k}_4)\, d\vec{k}_1\, d\vec{k}_2\, d\vec{k}_3\, d\vec{k}_4\\
&\quad + \frac{1}{4}\frac{1}{(2\pi)^2}\int D_{\vec{k}_1\vec{k}_2\vec{k}_3\vec{k}_4}(a_{\vec{k}_1}a_{\vec{k}_2}a^*_{\vec{k}_3}a^*_{\vec{k}_4}\delta(\vec{k}_1+\vec{k}_2-\vec{k}_3-\vec{k}_4)\, d\vec{k}_1\, d\vec{k}_2\, d\vec{k}_3\, d\vec{k}_4.
\end{aligned} \tag{8}$$

We omit formulae for matrix elements of these processes (they can be found in [18]) for the sake of conciseness.

For gravity waves on the surface of the deep fluid dispersion relation is $\omega_k = \sqrt{gk}$ and resonant conditions:

$$\omega_{k_0} = \omega_{k_1} + \omega_{k_2}, \qquad \vec{k}_0 = \vec{k}_1 + \vec{k}_2,$$

are never fulfilled, which means that three-waves processes of decaying and merging of the waves are prohibited. Such dispersion relations are of the "non-decay type".

In this case it is well known fact that cubic terms of the Hamiltonian (8) can be eliminated by proper canonical transformation $a(\vec{k}, t) \to b(\vec{k}, t)$. Hamiltonian in new variables looks as follows:

$$\begin{aligned}
H_0 &= \int \omega_k |b_{\vec{k}}|^2 d\vec{k},\\
H_1 &= 0,\\
H_2 &= \frac{1}{2}\frac{1}{(2\pi)^2}\int T_{\vec{k}_1\vec{k}_2\vec{k}_3\vec{k}_4} b^*_{\vec{k}_1} b^*_{\vec{k}_2} b_{\vec{k}_3} b_{\vec{k}_4} \delta(\vec{k}_1+\vec{k}_2-\vec{k}_3-\vec{k}_4) d\vec{k}_1 d\vec{k}_2 d\vec{k}_3 d\vec{k}_4.
\end{aligned}$$

The formula of the matrix element $T_{\vec{k}_1\vec{k}_2\vec{k}_3\vec{k}_4}$ is too bulky to give it here and can be found in [27].

If we suppose, that for our wave field phases and amplitudes are not correlated one can introduce pair correlator:

$$\left\langle a_{\vec{k}} a^*_{\vec{k}'} \right\rangle = n_k \delta(\vec{k} - \vec{k}'). \tag{9}$$

This is a hypothesis, although quite reasonable for the real sea surface. Even more, our observations show that initially not completely random spectrum (for example, with random phases but correlated amplitudes) become stochastic after several tens of charachteristic wave periods due to multiple nonlinear phase and amplitude mixing. We can verify it

by direct numerical simulation, but this question is out of the scope of present article. The $n_{\vec{k}}$ is measurable quantity, connected directly with observable correlation functions. For instance, from $a_{\vec{k}}$ definition one can get:

$$I_k = \left\langle |\eta_{\vec{k}}|^2 \right\rangle = \frac{1}{2}\frac{\omega_k}{g}(n_k + n_{-k}). \tag{10}$$

For gravity waves we can also use the following correlation function:

$$\left\langle b_{\vec{k}} b^*_{\vec{k}'} \right\rangle = N_k \delta(\vec{k} - \vec{k}'). \tag{11}$$

Because in the case of variables $b_{\vec{k}}$ all non-resonant processes are excluded this is the correlation function for which kinetic equation is derived.

The relation connecting n_k and N_k is very simple (in the case of deep water) [35]:

$$\frac{n_k - N_k}{n_k} \simeq \mu, \tag{12}$$

where $\mu = (ka)^2$, here a is a characteristic elevation of the free surface. In the case of the weak turbulence $\mu \ll 1$.

The correlation function N_k obeys the kinetic equation [15,33,41]:

$$\frac{\partial N_k}{\partial t} = S_{nl}(N, N, N) + S_{in}(k) - S_{diss}(k), \tag{13}$$

Here S_{in} corresponds to input of energy, S_{diss} is the dissipation of energy in the system, and

$$S_{nl}(N, N, N) = 4\pi \int \left| T_{\vec{k},\vec{k}_1,\vec{k}_2,\vec{k}_3} \right|^2 \times (N_{k_1} N_{k_2} N_{k_3} + N_k N_{k_2} N_{k_3} - N_k N_{k_1} N_{k_2} - N_k N_{k_1} N_{k_3})$$
$$\delta(\vec{k} + \vec{k}_1 - \vec{k}_2 - \vec{k}_3)\delta(\omega_k + \omega_{k_1} - \omega_{k_2} - \omega_{k_3})\, d\vec{k}_1\, d\vec{k}_2\, d\vec{k}_3, \tag{14}$$

describes nonlinear interaction of waves. Expression for $T_{\vec{k},\vec{k}_1,\vec{k}_2,\vec{k}_3}$ can be found in [27].

2.3. Kolmogorov–Zakharov solutions of kinetic equation

Let us consider stationary solutions of the kinetic equation assuming that:

- The medium is invariant with respect to rotations.
- Dispersion relation is a power-like function $\omega = ak^\alpha$.
- $T_{\vec{k},\vec{k}_1,\vec{k}_2,\vec{k}_3}$ is a homogeneous function: $T_{\varepsilon\vec{k},\varepsilon\vec{k}_1,\varepsilon\vec{k}_2,\varepsilon\vec{k}_3} = \varepsilon^\beta T_{\vec{k},\vec{k}_1,\vec{k}_2,\vec{k}_3}$.

Under these assumptions Zakharov [33,37,41,42] obtained Kolmogorov-like solutions corresponding to fluxes of two integrals of motion (energy and wave action or number of waves):

$$\begin{aligned} n_k^{(1)} &= C_1 P^{1/3} k^{-((2\beta/3)-d)}, \\ n_k^{(2)} &= C_2 Q^{1/3} k^{-(((2\beta-\alpha)/3)-d)}. \end{aligned} \tag{15}$$

Here d is a spatial dimension ($d = 2$ in our case). In the case of gravity waves on a deep water $\omega = \sqrt{gk}$ ($\alpha = 1/2$) and, apparently, $\beta = 3$. As a result one can get:

$$\begin{aligned} n_k^{(1)} &= C_1 P^{1/3} k^{-4}, \\ n_k^{(2)} &= C_2 Q^{1/3} k^{-23/6}. \end{aligned} \tag{16}$$

The first spectrum $n_k^{(1)}$ corresponds to the direct cascade, describing flux of energy from large scales (pumping) to small scales (dissipation). The second spectrum $n_k^{(2)}$ describes to inverse cascade, corresponding to flux of number of waves (or wave action) from small scales (pumping) to larger scales. In the case of swell or decaying turbulence inverse cascade reveals itself as a downshift of spectral maximum to smaller wavenumbers, resulting in growing long waves.

2.4. Verification of the kinetic equation

As it was shown during derivation of kinetic equation, we neglect some processes, such as multiple harmonics generation, because they are non-resonant. Also, statistical description by definition does not take into account rare or catastrophic events, for example solitons, freak wave formation, and wave breaking or whitecapping which could be very important. It means that we need to verify these assumptions using real life or numerical experiments.

Broad program of verification of kinetic equation for gravity waves was fulfilled during the last decade. The key method of verification is numerical simulation in the framework of primordial Hamiltonian equations for shape of the surface $\eta(\vec{r}, t)$ and velocity potential on the surface $\psi(\vec{r}, t)$. Such numerical experiments provide complete information about the system, including phase and amplitude of calculated function at every points of the surface at every moment of time. Of course such luxury comes at a great cost of enormous computational complexity. Due to rapid progress of computers available for computations and numerical algorithms during last couple of decades such simulations became possible. The first work which presented successful simulation of weak turbulence of gravity waves was published in the beginning of 2000s [25]. It was simulation of the decaying turbulence. Decaying turbulence experiments start from initial spectral distribution close to realistic swell which is propagating without pumping, decaying (loosing energy) due to nonlinear transfer from spectral peak to the dissipative scale. In the paper [25] formation of weak turbulent Kolmogorov–Zakharov [41] spectral tail was confirmed. In the series of works [11,12,18] the first confirmation of Kolmogorov–Zakharov spectra in systems with pumping was provided as well as confirmation of Independence of spectrum exponent from the pumping force in some reasonable interval of input fluxes. Shortly after that some possible obstacles for verification of Hasselmann equation through wave tank experiments were pointed out [39]. In papers [21,40] idea of modification of the dissipation term S_{diss} in order to take additional energy transfer to the dissipation scales due to whitecapping and wavebreaking was developed through a series of massive numerical simulations of decaying turbulence. In a recent paper [20] some consequences of whitecapping influence on a Kolmogorov–Zakharov spectra in wave tanks experiments were briefly analyzed.

3. Numerical simulation

3.1. Simulation parameters

Here we continue investigation of the problem which was started in [20]. We simulated the primordial dynamical equations (5) in a periodic spatial domain $2\pi \times 2\pi$. In order to save computation time multigrid approach has been used. Because formation of the inverse cascade is the most time consuming part of calculations (characteristic nonlinear time is about $\omega_k/\mu \simeq 10\omega_k$ and $\omega_k \sim \sqrt{k}$), we completed this calculation on the relatively small grid 256×256. After that we gradually increased resolution up to 1024×1024 nodes. To check whether we loose something in the high frequency region long time simulation on grid 256×256 was performed. It demonstrated absence of change in the inverse cascade, pumping and high frequencies region.

The used numerical code was verified in [10–12,21,39,40]. Gravity acceleration was $g = 1$. The pseudo-viscous damping coefficient had the following form:

$$\gamma_k = \begin{cases} \gamma_0 (k - k_d)^2, & \text{if } k > k_d, \\ 0, & \text{if } k \le k_d; \end{cases} \tag{17}$$

where $k_d = 256$ and $\gamma_{0,1024} = 2.7 \times 10^4$ for the 1024×1024 grid and $k_d = 64$ and $\gamma_{0,256} = 2.4 \times 10^2$ for the smaller 256×256 grid. Pumping was an isotropic driving force narrow in wavenumber space with random phase:

$$P_{\vec{k}} = f_k e^{i R_{\vec{k}}(t)}, \quad f_k = \begin{cases} 4F_0 \dfrac{(k - k_{p1})(k_{p2} - k)}{(k_{p2} - k_{p1})^2}, \\ 0 \quad \text{if } k < k_{p1} \text{ or } k > k_{p2}; \end{cases} \tag{18}$$

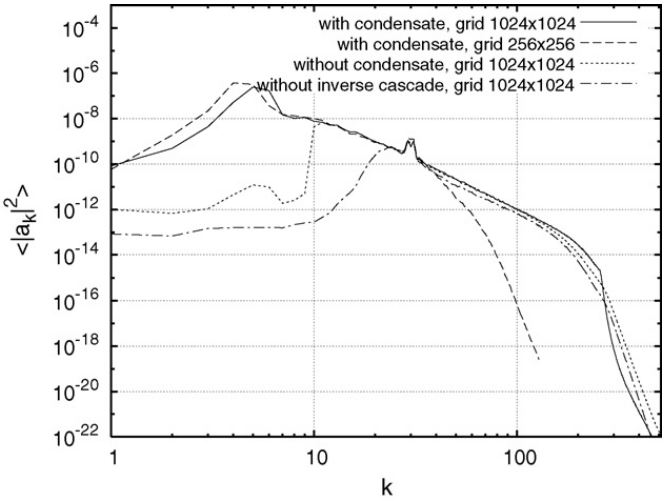

Fig. 1. Spectra $\left\langle |a_k|^2 \right\rangle$. With condensate on the 1024×1024 grid (solid); on the 256×256 grid with more developed condensate (dashed); without condensate on the 1024×1024 grid (dotted); without inverse cascade on the 1024×1024 grid (dashed-dotted).

here $k_{p1} = 28$, $k_{p2} = 32$ and $F_0 = 1.5 \times 10^{-5}$; $R_{\vec{k}}(t)$ was a uniformly distributed random number in the interval $(0,2\pi]$ for each $\vec{k}$ and t. The initial condition was low amplitude noise in all harmonics. Time steps were $\Delta t_{1024} = 6.7 \times 10^{-4}$ and $\Delta t_{256} = 5.0 \times 10^{-3}$. We used Fourier series in the following form:

$$\eta_{\vec{k}} = \hat{F}[\eta_{\vec{r}}] = \frac{1}{(2\pi)^2} \int_0^{2\pi} \int_0^{2\pi} \eta_{\vec{r}} e^{i\vec{k}\vec{r}} d^2 r, \qquad \eta_{\vec{r}} = \hat{F}^{-1}[\eta_{\vec{r}}] = \sum_{-N_x/2}^{N_x/2-1} \sum_{-N_y/2}^{N_y/2-1} \eta_{\vec{k}} e^{-i\vec{k}\vec{r}}.$$

3.2. Results

As it was reported in [20] as a result of simulation we observed formation of both direct and inverse cascades (Fig. 1, solid line), although exponents of power-like spectra were different from weak turbulent solutions (16). It is important to note that development of the inverse cascade spectrum was arrested by the discreteness of the wavenumber grid in agreement with [10,17,23,39]. After that, a large scale condensate started to form. The reason of this phenomenon is the following. It can be shown that resonant conditions for four-waves interaction of gravity waves are never fulfilled exactly on the discrete grid of wavevectors (integer number for $2\pi \times 2\pi$ box):

$$\omega_{k_1} + \omega_{k_2} - \omega_{k_3} - \omega_{k_4} \neq 0.$$

Nonlinear frequency shift Γ weakens resonant condition, now resonant curve has finite width:

$$|\omega_{k_1} + \omega_{k_2} - \omega_{k_3} - \omega_{k_4}| \leq \Gamma.$$

Nonlinear frequency shift depends on $T_{\vec{k}_1\vec{k}_2\vec{k}_3\vec{k}_4}$, which is homogeneous function. It grows as k_3 when k is increased. This is the reason why it is much easier to get resonant interaction in the direct cascade region (high wavenumbers). It also decreases as k_3 when $k \to 0$. It means that effectively grid become more and more coarse at large scales. It means that at some scale inverse cascade is stopped because four-waves nonlinear interaction is "turned off". At the same time flux of action still brings new waves to this scale. We have "condensation" [9] of waves. Similar processes were observed in 2D-hydrodynamics [5] and plasma [28]. It is worth to mention, that the same mechanism provides broadening of the resonant curve in the high wavenumbers. As a result, the finest numerical grid in our experiment (1024×1024) is definitely beyond the threshold which secures resonant interactions for high frequencies (high-$\vec{k}$) modes of direct cascade. Reasonable results were obtained already on the grid 256×256 in [11] and universality was confirmed later in [12].

As one can see, the value of wave action $\left\langle |a_k|^2 \right\rangle$ at the condensate region is more than an order of magnitude higher than for the closest harmonic of the inverse cascade. The dynamics of large scales became extremely slow after this

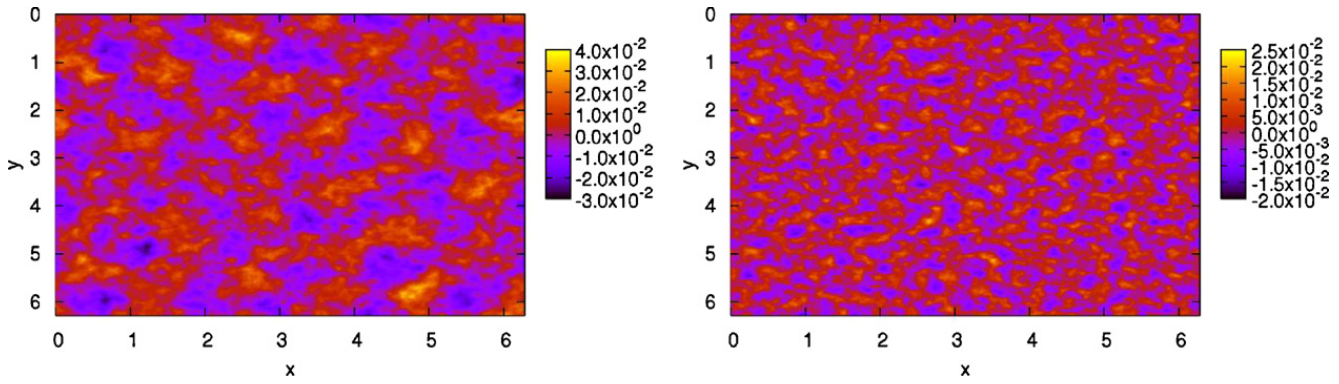

Fig. 2. Surface of the fluid $\eta(\vec{r})$ with (left) and without (right) condensate.

point. We managed to achieve downshift of the condensate peak by one step of the wavenumber grid during long time simulation on a small grid (256×256) (Fig. 1, line with long dashes). As one can see, we observed elongation of the inverse cascade interval without significant change of the slope. Unfortunately, the inertial interval for inverse cascade was too short to exclude the possible influence of pumping and condensate.

The question whether these spectra are stationary or not is still open. It was nearly impossible to understand this from the numerical results. Spectrum of inverse cascade was growing very slowly, which resulted in further propagation of the condensate by one step in $\vec{k}$-space. A the same time, after the grid was increased and we got direct cascade tail, spectrum was visually stabilized. We were unable to observe any significant change during several hundreds of periods of peak wave. The hypothesis is that due to condensate stimulated whitecapping we have "friction" of condensate and small scale waves (mechanism is described below) which leads effectively to drain of wave action from the region of large scales and stabilization of the spectrum. The confirmation of this hypothesis requires long time simulations in order to compare directly the results obtained on small grid and on large grid at the same moment of time. This simulations are hardly possible with available code and are definitely out of scope of the current article.

For direct cascade spectra we also used a log–log scale. Results are present in Fig. 3 (left). Formally, in this case we have quite a long inertial interval $32 < k < 256$, but in reality damping has an influence on the spectrum approximately up to $k \simeq 180$. Nevertheless, in this case we have more than half of a decade in $\vec{k}$-space. The theory of weak turbulence gives us dependence $\sim k^{-4}$ (16), known as Kolmogorov–Zakharov direct cascade spectrum for gravity waves. Nevertheless, one can see that we observe $k^{-9/2}$, known as Phillips [26,24] spectrum. Possible explanation was provided in [20]. The main idea was the following: presence of the condensate stimulated additional whitecapping and wavebreaking processes by local increase of steepness. These processes provide additional transfer of energy to the dissipation region. When this dissipation is strong enough to balance flux of energy, such mechanism should give Phillips spectrum as a result [24]. The detailed analysis of the fluxes and their balance is a topic of separate work. In order to estimate dissipation due to whitecapping we need to know at least dependence of dissipation function on average steepness. Our recent findings [38] show that we cannot use currently available empirical formulae. At the same time, value of the dimensionless Phillips constant 10^{-3} is consistent with the results of experimental observations given in [32]. It was shown, that suppression of the condensate (see Fig. 2) changes spectrum exponent to some value closer to the theory of weak turbulence. However, at that time we failed to avoid long waves' influence on the direct cascade spectrum completely. The longest waves of inverse cascade were providing long wave background which influence distorted the spectrum.

In order to eliminate this influence let us suppress inverse cascade completely by artificial damping in low wavenumbers. The result of simulation is shown in Fig. 3 (right panel).

For comparison we have put in the same figure initial spectrum for direct cascade (left). As one can see, the exponent of the spectrum changed and now almost coincides with the prediction of the weak turbulent theory. The tiny difference may be a result of the influence of the left peak, which is the result of insufficient length of damping region. At the same time, longer artificial damping can start to influence the pumping area and change the input flux significantly.

3.3. Discussion and explanation

A qualitative explanation of the condensate's influence on the short waves could be the following: let us consider a propagating wave with some given slope at its front; a much longer wave can be treated as a presence of a strong

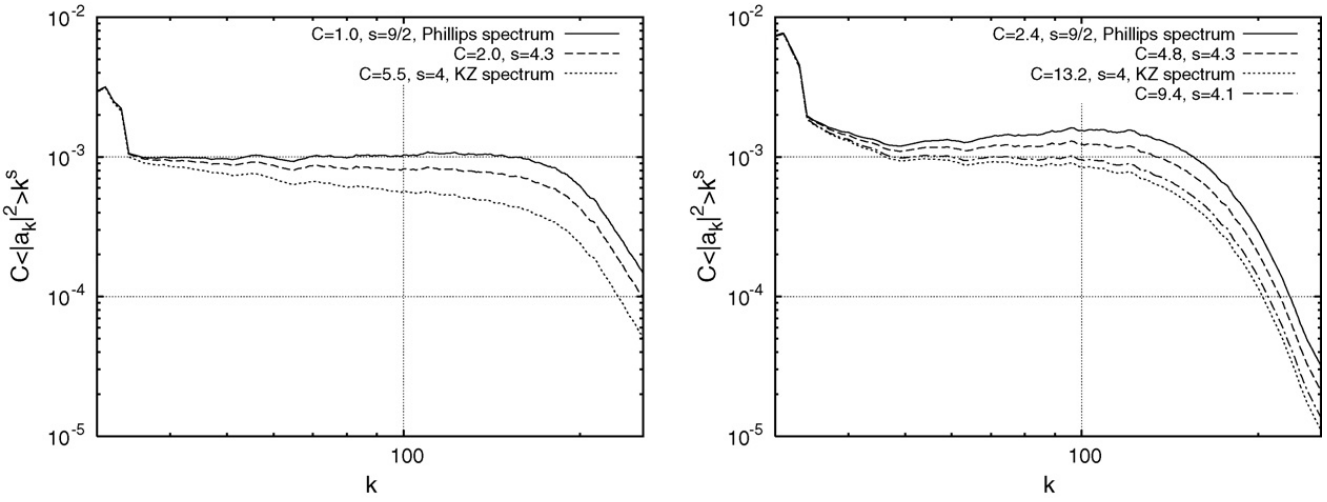

Fig. 3. Compensated direct cascade spectra $C\left\langle |a_k|^2 \right\rangle k^s$ with condensate and inverse cascade (left) and without them (right).

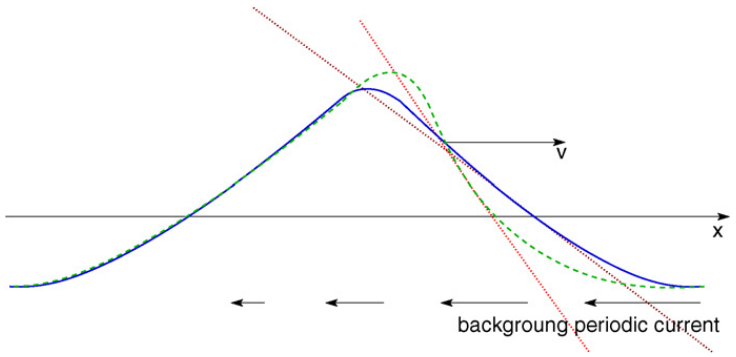

Fig. 4. Initial wave (solid line) become steeper (dashed line) in the result of interaction with the background current.

background flow. If the direction of the flow is opposite to direction of the wave's propagation (it always happens somewhere on the surface at least in the case of isotropic turbulence), the slope of the wave's front will increase (see Fig. 4). This is what we see in our simulations. The average steepness $\mu = \sqrt{\left\langle |\vec{\nabla}\eta|^2 \right\rangle}$ has changed: with condensate $\mu_c \simeq 0.14$ (Fig. 5), without condensate $\mu_{nc} \simeq 0.12$ (Fig. 6), after suppression of inverse cascade $\mu_{nc} \simeq 0.1$ (Fig. 7). We should mention that very high values of gradient of the surface (higher that value for a limiting Stokes wave) are possible in our model only due to very strong damping at high wavenumbers and relatively narrow inertial interval, which prevents waves from real breaking by strong dissipation of energy for every breaking onset. We regularize our model by this dissipation. At the same time here we do not need to know details of the energy dissipation (how in details wave breaks and produce very short waves), all we need is to dissipate all the energy involved in the breaking.

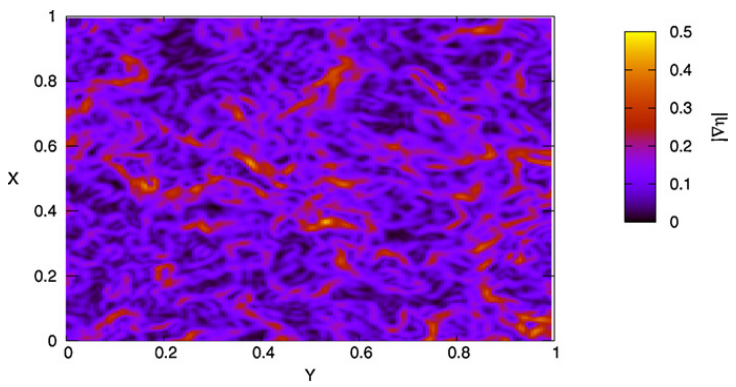

Fig. 5. Gradient of some part of the surface. In the presence of condensate.

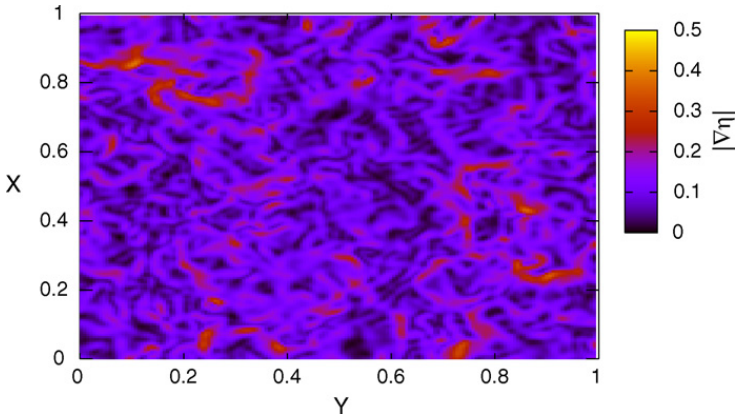

Fig. 6. Gradient of some part of the surface. In the absence of condensate.

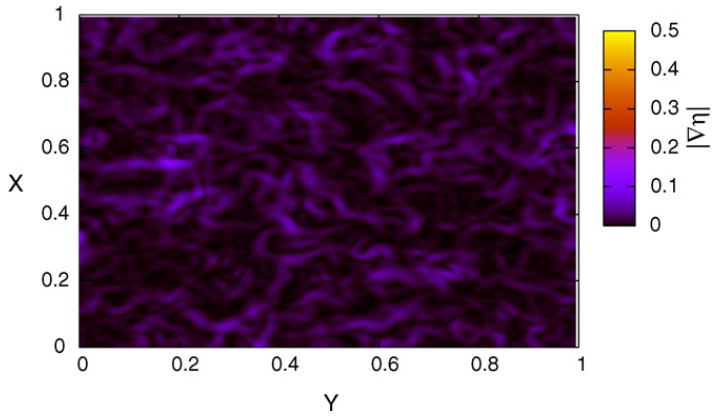

Fig. 7. Gradient of some part of the surface. In the absence of inverse cascade.

4. Conclusion

The observed phenomena of condensate formation and its influence on the direct cascade have to be quite common for experiments in experimental wave tanks. Finite size of the surface area gives us the same discrete grid of wavevectors as in the case of periodic boundary conditions. It means that at some large scale four-waves nonlinear interaction will be arrested, which provides conditions for condensate formation due to flux corresponding to inverse cascade. Such condensate will distort the direct cascade spectrum, changing its exponent through stimulation of whitecapping, resulting in additional dissipation. It is worth to note that this is threshold phenomenon with respect to average steepness as it was shown in [4]. If such dissipation is strong enough to balance the flux of energy, following [24] we shall get Phillips spectrum, as it was demonstrated in the present paper. Gradually suppressing condensate and inverse cascade one can achieve spectrum corresponding to the stationary solution of the kinetic equation. Simple mechanism of condensate interaction with short waves of direct cascade was proposed. This interaction along with other distortion possibilities (see, for example, [19]) can be the reason of observed spectra deviation from the weak turbulence predictions. These results can be used for explanation of experimental data obtained in the wave tanks.

Acknowledgments

The author would like to thank V.E. Zakharov, V.V. Lebedev, and I.V. Kolokolov for fruitful discussions.

This work was partially supported by RFBR grants 09-01-00631-a, 07-01-92165-NCNI-a Federal Targeted Program of the Russian Federation “S&S PPIR”, the Program “Fundamental problems of nonlinear dynamics” from the RAS Presidium and “Leading Scientific Schools of Russia” grant NSh-6885.2010.2.

The author would also like to thank the creators of the free open-source fast Fourier transform library FFTW [14] for this fast, cross platform, and reliable software.

References

[1] S.Y. Annenkov, V.I. Shrira, Direct numerical simulation of downshift and inverse cascade for water wave turbulence, Phys. Rev. Lett. 96 (2006) 204501.
[2] S.I. Badulin, A.V. Babanin, D. Resio, V.E. Zakharov, Weakly turbulent laws of wind-wave growth, J. Fluid Mech. 591 (2007) 339–378.
[3] S.I. Badulin, A.N. Pushkarev, D. Resio, V.E. Zakharov, Self-similarity of wind-driven seas, Nonlinear Proc. Geophys. 12 (2005) 891–946.
[4] M.L. Banner, A.V. Babanin, I.R. Young, Breaking probability for dominant waves on the sea surface, J. Phys. Oceanogr. 30 (2000) 3145–3160.
[5] M. Chertkov, C. Connaughton, I.V. Kolokolov, V.V. Lebedev, Dynamics of energy condensation in two-dimensional turbulence, Phys. Rev. Lett. 99 (2007) 084501.
[6] P. Denissenko, S. Lukaschuk, S.V. Nazarenko, Gravity wave turbulence in a laboratory flume, Phys. Rev. Lett. 99 (2007) 014501.
[7] F. Dias, A.I. Dyachenko, V.E. Zakharov, Theory of weakly damped free-surface flows: a new formulation based on potential flow solutions, Phys. Lett. A 372 (8) (2008) 1297–1302.
[8] M.A. Donelan, J. Hamilton, W.H. Hui, Directional spectra of wind generated waves, Phil. Trans. R. Soc. Lond. A315 (1985) 509.
[9] A.I. Dyachenko, G. Falkovich, Condensate turbulence in two dimensions, Phys. Rev. E 54 (1996) 5095–5099.
[10] A.I. Dyachenko, A.O. Korotkevich, V.E. Zakharov, Decay of the monochromatic capillary wave, JETP Lett. 77 (9) (2003) 477–481.
[11] A.I. Dyachenko, A.O. Korotkevich, V.E. Zakharov, Weak turbulence of gravity waves, JETP Lett. 77 (10) (2003) 546–550.
[12] A.I. Dyachenko, A.O. Korotkevich, V.E. Zakharov, Weak turbulent kolmogorov spectrum for surface gravity waves, Phys. Rev. Lett. 92 (13) (2004) 134501.
[13] E. Falcon, S. Fauve, C. Laroche, Observation of intermittency in wave turbulence, Phys. Rev. Lett. 98 (2007) 154501.
[14] M. Frigo, S.G. Johnson, The design and implementation of fftw 3, Proc. IEEE 93 (2) (2005) 216–231, http://fftw.org.
[15] K. Hasselmann, On the non-linear energy transfer in a gravity-wave spectrum part 1. General theory, J. Fluid Mech. 12 (4) (1962) 481–500.
[16] P.A. Hwang, D.W. Wang, E.J. Walsh, W.B. Krabill, R.N. Swift, Airborne measurements of the wavenumber spectra of ocean surface waves. Part i. Spectral slope and dimensionless spectral coefficient, J. Phys. Oceanogr. 30 (2007) 2753–2767.
[17] E. Kartashova, S.V. Nazarenko, O. Rudenko, Resonant interactions of nonlinear water waves in a finite basin, Phys. Rev. E 78 (2008) 016304.
[18] A.O. Korotkevich, Numerical simulation of weak turbulence of surface waves, Ph.D. Thesis, L.D. Landau Institute for Theoretical Physics, Moscow-Chernogolovka, Russia, 2003.
[19] A.O. Korotkevich, On the doppler distortion of the sea-wave spectra, Physica D 237 (21) (2008) 2767–2776.
[20] A.O. Korotkevich, Simultaneous numerical simulation of direct and inverse cascades in wave turbulence, Phys. Rev. Lett. 101 (7) (2008) 074504.
[21] A.O. Korotkevich, A. Pushkarev, D. Resio, V.E. Zakharov, Numerical verification of the weak turbulent model for swell evolution, Eur. J. Mech. B: Fluids 27 (4) (2008) 361–387.
[22] Y. Lvov, S.V. Nazarenko, B. Pokorni, Discreteness and its effect on water-wave turbulence, Physica D 99 (1) (2006) 24–35.
[23] S.V. Nazarenko, Sandpile behaviour in discrete water-wave turbulence, J. Stat. Mech. (2006) L02002.
[24] A.C. Newell, V.E. Zakharov, The role of the generalized phillips' spectrum in wave turbulence, Phys. Lett. A 372 (2008) 4230–4233.
[25] M. Onorato, A.R. Osborne, M. Serio, D. Resio, A. Pushkarev, V.E. Zakharov, C. Brandini, Freely decaying weak turbulence for sea surface gravity waves, Phys. Rev. Lett. 89 (2002) 144501.
[26] O.M. Phillips, The equilibrium range in the spectrum of wind-generated ocean waves, J. Fluid Mech. 4 (1958) 426–434.
[27] A. Pushkarev, D. Resio, V.E. Zakharov, Weak turbulent approach to the wind-generated gravity sea waves, Physica D 184 (2003) 29–63.
[28] M.G. Shats, H. Xia, H. Punzmann, G. Flakovich, Suppression of turbulence by self-generated and imposed mean flows, Phys. Rev. Lett. 99 (2007) 164502.
[29] M. Tanaka, Verification of hasselmann's energy transfer among surface gravity waves by direct numerical simulations of primitive equations, J. Fluid Mech. 444 (2001) 199–221.
[30] Y. Toba, Local balance in the air–sea boundary processes iii: on the spectrum of wind generated waves, J. Oceanogr. 29 (1973) 209–220.
[31] N. Yokoyama, Statistics of gravity waves obtained by direct numerical simulation, J. Fluid Mech. 501 (2004) 169–178.
[32] I.R. Young, Wind Generated Ocean Waves, Elsevier, Amsterdam, Oxford, 1999.
[33] V.E. Zakharov, On the theory of surface waves, Ph.D. Thesis, Budker Institute for Nuclear Physics, Novosibirsk, USSR, 1967.
[34] V.E. Zakharov, Stability of periodic waves of finite amplitude on a surface, J. Appl. Mech. Tech. Phys. 9 (1968) 190–194.
[35] V.E. Zakharov, Statistical theory of gravity and capillary waves on the surface of a finite-depth fluid, Eur. J. Mech. B: Fluids 18 (3) (1999) 327–344.
[36] V.E. Zakharov, Theoretical interpretation of fetch limited wind-driven sea observations, Nonlinear Proc. Geophys. 12 (2005) 1011–1020.
[37] V.E. Zakharov, N.N. Filonenko, Energy spectrum for stochastic oscillations of the surface of a liquid, Sov. Phys. Dokl. 11 (1967) 881–884.
[38] V.E. Zakharov, A.O. Korotkevich, A.O. Prokofiev, On dissipation function of ocean waves due to whitecapping, AIP Proc. CP1168 2 (2009) 1229–1231.
[39] V.E. Zakharov, A.O. Korotkevich, A. Pushkarev, A.I. Dyachenko, Mesoscopic wave turbulence, JETP Lett. 82 (8) (2005) 487–491.
[40] V.E. Zakharov, A.O. Korotkevich, A. Pushkarev, D. Resio, Coexistence of weak and strong wave turbulence in a swell propagation, Phys. Rev. Lett. 99 (16) (2007) 164501.
[41] V.E. Zakharov, V.S. Lvov, G. Falkovich, Kolmogorov Spectra of Turbulence I, Springer-Verlag, Berlin, 1992.
[42] V.E. Zakharov, M.M. Zaslavskii, The kinetic equation and kolmogorov spectra in the weak turbulence theory of wind waves, Izv. Atmos. Ocean. Phys. 18 (1982) 747–753.